J Mater Sci (2009) 44:4834–4839
DOI 10.1007/s10853-009-3737-8

Microwave-hydrothermal synthesis of nano-sized Sn^{2+}-doped $BaTiO_3$ powders and dielectric properties of corresponding ceramics obtained by spark plasma sintering method

Yahong Xie · Shu Yin · Takatoshi Hashimoto · Hisamichi Kimura · Tsugio Sato

Received: 20 January 2009 / Accepted: 9 July 2009 / Published online: 23 July 2009

Abstract Ternary oxides containing Sn^{2+} are rare and difficult to prepare using solid state reaction due to disproportionation of Sn^{2+} at high temperature. In this paper, nanoparticles of barium titanate doped with different amounts of Sn^{2+} consisting of single phase perovskite structure were successfully synthesized for the first time by using a microwave-assisted solvothermal reaction. The particle sizes were about 20–40 nm in diameter and increased with increasing the amount of doped tin. Solidified ceramic bodies were obtained using a spark plasma sintering method under argon atmosphere avoiding the disproportionation and oxidation of Sn^{2+} in the air. The grain size and dielectric constant of the sintered body decreased with increasing the amount of doped tin.

Introduction

The physicochemical properties of Sn^{2+} compounds are interesting because of their unique properties such as visible light responsive photocatalyst and piezoelectric properties [1–3]. Moreover, $SnTiO_3$ has been estimated to show excellent ferroelectric properties similar to those of $PbTiO_3$ by first principle calculations. However, it is impossible to prepare $SnTiO_3$ using conventional ceramic processing routes due to the disproportionation of Sn^{2+} at high temperature [4–10]. On the other hand, $BaTiO_3$, a well-known lead-free dielectric and piezoelectric material [11, 12], can be synthesized by using various kinds of methods. Therefore, Sn^{2+}-doped $BaTiO_3$ were attempted to be synthesized in this paper.

Instead of conventional ceramic processing routes, the microwave-assisted solvothermal reaction, which has been recognized as an energy and time saving process with faster kinetics of crystallization, seems to be one of the best ways to realize the low-temperature synthesis of Sn^{2+}-doped $BaTiO_3$ [13–17]. To avoid further disproportionation of Sn^{2+} during the sintering, a spark plasma sintering (SPS), by which ceramics can be sintered very rapidly to full density under an inert gas atmosphere, seems to be an effective sintering method for Sn^{2+}-doped $BaTiO_3$. In this method, the powder in a carbon die is pressed uniaxially and direct current pulse voltage is applied. As a result, the sample can be sintered uniformly and rapidly from both inside and outside [18, 19].

In this work, Sn^{2+}-doped $BaTiO_3$ was synthesized and sintered under mild temperatures. The doping of tin resulted in decreasing the grain size, and dielectric constant of the products were investigated.

Experimental

Microwave-hydrothermal synthesis

Reagent grade $BaCl_2$, $SnCl_2{\cdot}2H_2O$ and $Ti(i\text{-}C_3H_7O)_4$ were used as starting materials. Initially, a 10 cm^3

Y. Xie (✉) · S. Yin · T. Sato
Institute of Multidisciplinary Research for Advanced Materials (IMRAM), Tohoku University, Sendai 980-8577, Japan
e-mail: xyh0707@hotmail.com

T. Hashimoto
NEC Tokin Corporation, Koriyama, Taihaku-ku, Sendai 980-8510, Japan

H. Kimura
Institute of Material Research, Tohoku University, Sendai 980-8577, Japan

portion of 0.5 M $SnCl_2$–$BaCl_2$ mixed aqueous solution and a 10 cm^3 portion of 0.5 M Ti(i-$C_3H_7O)_4$ i-propanol solution were mixed under stirring, then a desired amount of KOH solution was added into the mixture, in which the molar ratio of (Sn + Ba)/Ti was fixed at 1:1. Then, the suspended solution was diluted with water to 30 cm^3 and transferred to a Teflon reaction vessel of 70 cm^3 of internal volume and then was irradiated by microwave to start the solvothermal reaction at 200 °C for 1 h using a microwave reaction apparatus (ACTAC Co., MWS-2). After reaction, the precipitate was collected with a centrifuge and rinsed with ethanol, deionized water and acetone three times, respectively. Then, the obtained powders were dried overnight at 60 °C in a vacuum oven.

The SPS process

The SPS process was carried out by using spark plasma sintering system (DR.SINTER^{TM}). The powder was put into a carbon die with an inner diameter of 30 mm and heated up to a certain temperature at a heating rate of 600 °C/min and applying a pressure of 40 MPa under argon atmosphere with monitoring the shrinkage of the sample. When the shrinkage rate decreased, the heating rate was slowed down and finally when the shrinkage rate became negligibly small, the temperature was kept constant for a certain period of time. After that the pressure was released and the sample was cooled to room temperature to get the sintered sample pellets of 30 mm in diameter and ca. 2.5 mm in height. The densities of the samples were measured by using the Archimedes method.

For comparison, pure $BaTiO_3$ ceramic bodies with different densities were prepared at different sintering temperatures.

Characterization

Thermogravimetric analysis (TG-DTA, Rigaku, TG8101D) was performed for powders from room temperature to 1200 °C with a heating rate of 10 °C/min in air. The particle morphology was observed by using a transmission electron microscopy (JEOL, JEM-2000EX), and the X-ray diffraction (XRD) analysis of the obtained powder samples was carried out using CuKα radiation with a pyrolytic graphite monochromator mounted on a powder diffractometer (Shimadzu XD-D1). The particle morphology was observed by using a transmission electron microscopy (JEOL, JEM-2000EX) and the microstructures of the solidified compacts were observed using a scanning electron microscope (SEM; Hitachi S-4100). The dielectric properties were measured using Agilent 4294A precision impedance analyzer.

Results and discussion

Crystalline phase

The XRD patterns of the samples of $BaTiO_3$, $Ba_{0.9}Sn_{0.1}TiO_3$ and $Ba_{0.8}Sn_{0.2}TiO_3$ obtained at 200 °C for 1 h with the concentration of KOH of 0.9 M via a microwave-assisted solvothermal reaction are shown in Fig. 1. All the diffraction peaks were identified with the cubic perovskite type $BaTiO_3$ and no other second phase was observed. The lattice parameters obtained by XRD analysis are tabulated

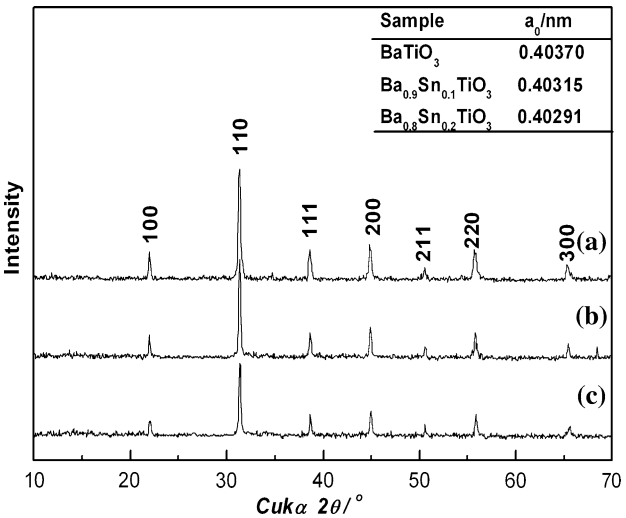

Fig. 1 XRD patterns of (a) $BaTiO_3$, (b) $Ba_{0.9}Sn_{0.1}TiO_3$ and (c) $Ba_{0.8}Sn_{0.2}TiO_3$

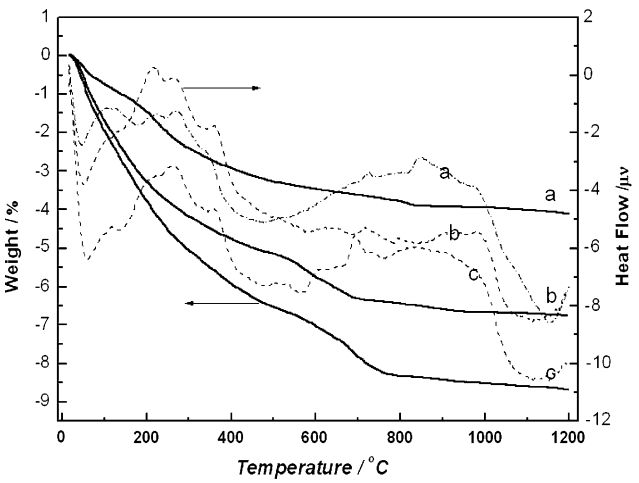

Fig. 2 TG-DTA curves of (a) $BaTiO_3$, (b) $Ba_{0.90}Sn_{0.10}TiO_3$ and (c) $Ba_{0.80}Sn_{0.20}TiO_3$

inside the figure, indicating that the lattice constant decreases with increasing the amount of Sn^{2+}. These results suggest that Sn^{2+} locates at not Ti^{4+} site but Ba^{2+} in the perovskite structure, since the ionic size of Sn^{2+} is larger than that of Ti^{4+} but smaller than that of Ba^{2+} resulting in the decrease of lattice parameters.

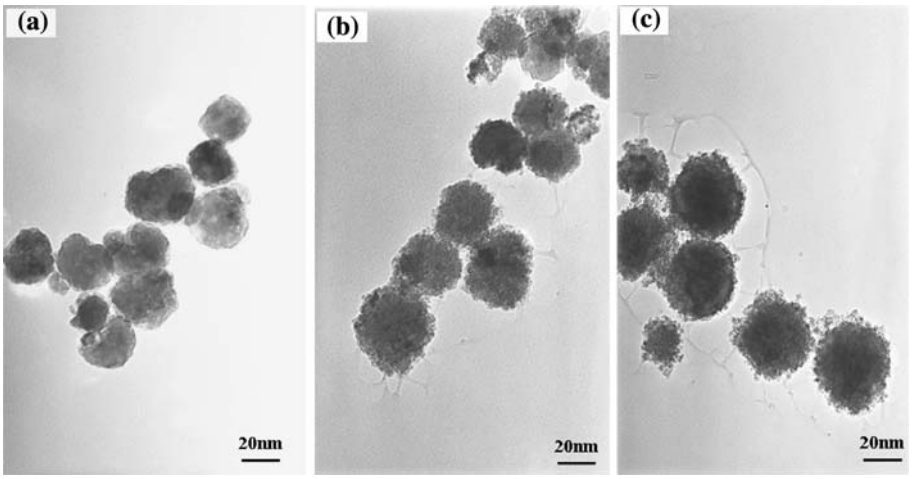

Fig. 3 TEM images of **a** $BaTiO_3$, **b** $Ba_{0.90}Sn_{0.10}TiO_3$ and **c** $Ba_{0.80}Sn_{0.20}TiO_3$ powders

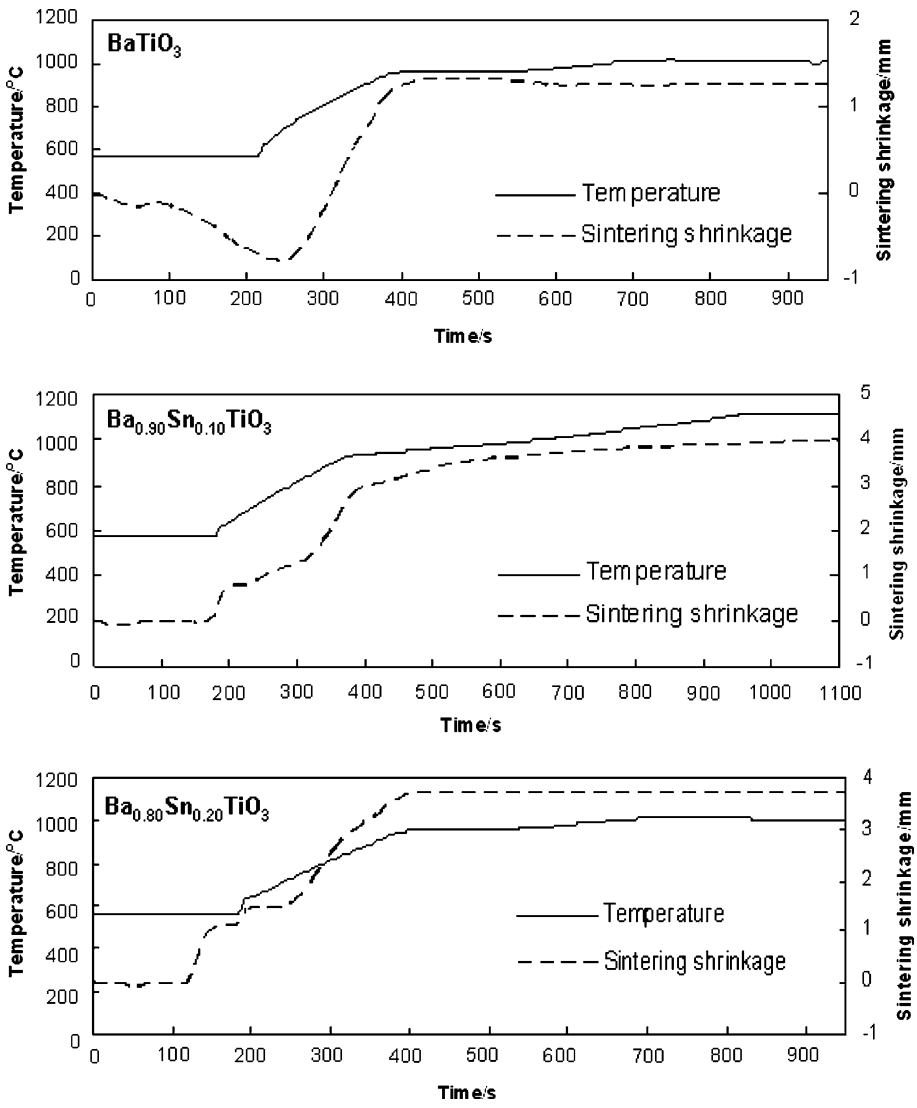

Fig. 4 Temperature and sintering shrinkage profiles of samples with time during a SPS process

Thermal stability of the perovskite-type synthesized compound

Figure 2 shows the TG-DTA curves of the $BaTiO_3$ doped with different amounts of Tin(II). All samples showed weight losses up to around 800 °C and then the weights were almost constant. Generally, the weight loss of the sample prepared by solution process from room temperature to around 200 °C attributed to the loss of adsorbed water. Therefore, the endothermic peaks observed from room temperature to 200 °C seemed to be due to the loss of the adsorbed water and/or *i*-propanol and those from 250 to 800 °C may be due to the dehydration from OH group in the lattice. It can be seen that the weight loss increased with increasing the amount of doped tin, i.e., the total weight loss amounts to 4.1, 6.6 and 8.5% for $BaTiO_3$, $Ba_{0.9}Sn_{0.1}TiO_3$ and $Ba_{0.8}Sn_{0.2}TiO_3$, respectively, indicating that the amount of OH group incorporated in the lattice increased with increasing the amount of Sn^{2+} doped in the lattice.

Morphology of the obtained powders

From the TEM images (Fig. 3), it can be observed that all of the prepared samples, $BaTiO_3$, $Ba_{0.9}Sn_{0.1}TiO_3$ and $Ba_{0.8}Sn_{0.2}TiO_3$, consisted of spherical nanoparticles with the particle size from 20 to 40 nm. It seemed that the particle size increased and crystallinity decreased with increasing the amount of doped Sn^{2+}. We do not exactly know the reasons of such change on the morphology and crystallinity of the grains. One can suppose that the doped Sn^{2+} segregates at grain boundaries, which would decrease the crystallinity of the particles [20–22].

Morphology of the ceramic body obtained by using SPS method

Figure 4 shows the temperature and sintering shrinkage profiles of the samples with time during the SPS process. All samples were heated to ca. 1000 °C within 200 s and final sintering temperatures of $BaTiO_3$, $Ba_{0.9}Sn_{0.1}TiO_3$ and $Ba_{0.8}Sn_{0.2}TiO_3$ were 1000, 1100 and 1020 °C, respectively. The total time required for SPS process was less than 1100 s. The densities of the sintered bodies of $BaTiO_3$, $Ba_{0.9}Sn_{0.1}TiO_3$ and $Ba_{0.8}Sn_{0.2}TiO_3$ were 5.92, 5.48 and 5.11 g cm^{-3}, respectively. It was seen that the degrees of shrinkage of $Ba_{0.9}Sn_{0.1}TiO_3$ and $Ba_{0.8}Sn_{0.2}TiO_3$ were much larger than that of $BaTiO_3$, indicating that the packing densities of $Ba_{0.9}Sn_{0.1}TiO_3$ and $Ba_{0.8}Sn_{0.2}TiO_3$ powders were much lower than that of $BaTiO_3$. These results agreed with the TEM observation (Fig. 3) that the crystallinity of the sample decreased with increasing the Sn^{2+} content.

Figure 5 shows the typical SEM photographs of the fractured surfaces of the $Ba_{1-x}Sn_xTiO_3$ specimens sintered at 1100 °C using SPS method under argon atmosphere. The grain size significantly decreased from 1 μm to 100 nm when the Tin(II) content increased from 0 to 20%, while the grain morphology varied polyhedron to spherical, indicating that the sintering was depressed by doping with Tin(II).

Phase of the obtained ceramic body

Figure 6 shows the XRD patterns of the sintered bodies of $BaTiO_3$, $Ba_{0.9}Sn_{0.1}TiO_3$ and $Ba_{0.8}Sn_{0.2}TiO_3$. All peaks could

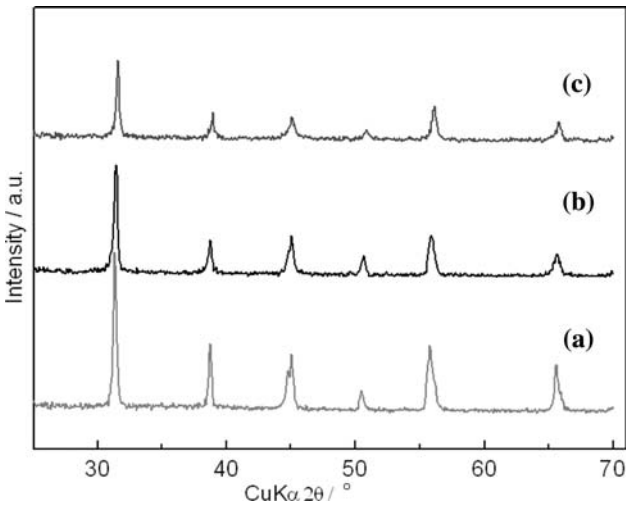

Fig. 6 XRD patterns of the obtained ceramic body of (a) $BaTiO_3$, (b) $Ba_{0.9}Sn_{0.1}TiO_3$ and (c) $Ba_{0.8}Sn_{0.2}TiO_3$

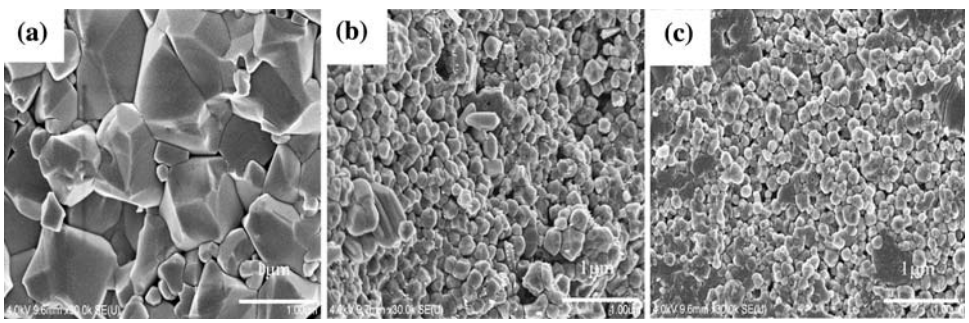

Fig. 5 SEM images of **a** $BaTiO_3$, **b** $Ba_{0.90}Sn_{0.10}TiO_3$ and **c** $Ba_{0.80}Sn_{0.20}TiO_3$ ceramic body

Table 1 Dielectric properties of the obtained ceramic body

SPS	Body density	Dielectric constant	s_{33} (E/pm^2/N)	k_{33}	d_{33} (pc/N)
$BaTiO_3$	5.92 (98.4%)	2937	11.2	36%	209
$Ba_{0.90}Sn_{0.10}TiO_3$	5.48 (91.2%)	1421	Cannot be polarized		
$BaTiO_3$[a]	5.47 (91.0%)	1892			
$Ba_{0.80}Sn_{0.20}TiO_3$	5.11 (85.1%)	1201	Cannot be polarized		
$BaTiO_3$[b]	5.10 (85.0%)	1657			
BT literature data, calcined at 1240 °C [24]	5.70 (94.8%)	4200			170

[a] $BaTiO_3$: prepared at 1200 °C for 5 h using conventional sintering method

[b] $BaTiO_3$: prepared at 1150 °C for 5 h using conventional sintering method

be attributed to perovskite-type $BaTiO_3$ and no other impurity phase appeared. Thus, the SPS method under an inert gas atmosphere is considered to be suitable for the sintering of Sn^{2+}-doped $BaTiO_3$ by avoiding the disproportionation reaction of Sn^{2+} at high temperature. From the splitting of the peak around 45° it seemed that the $BaTiO_3$ ceramic consisted of the mixture of cubic phase and tetragonal phase.

Dielectric property

It is known that the dielectric property is heavily dependent on the relative density and grain size of the samples [23]. Table 1 shows the dielectric properties of obtained $BaTiO_3$, $Ba_{0.9}Sn_{0.1}TiO_3$ and $Ba_{0.8}Sn_{0.2}TiO_3$ ceramics. The relative density decreased with increasing the amount of doped Sn^{2+} from 98.4 to 85.1%, correspondingly the dielectric constant decreased as 2937, 1421 and 1201 for $BaTiO_3$, $Ba_{0.9}Sn_{0.1}TiO_3$ and $Ba_{0.8}Sn_{0.2}TiO_3$, respectively. Piezoelectric ceramics is a kind of material which produces an electrical charge when a load is applied and deformation occurs, d_{33} (piezoelectric charge constant) represents a relationship between signal of electrical chare and deformation. The d_{33} value of synthesized $BaTiO_3$, 209, is larger than literature data, 170 (see Table 1), which may be attributed to the high sintering density, 98.4% theoretical of and $BaTiO_3$ and appropriate grain size. The doped samples could not be polarized, which can be understood by considering that the substitution of Sn^{2+} ions in Ba^{2+} positions results in the increase of the symmetry in crystal structure to decrease the dielectric properties. Furthermore, low sintering density is also attributed to the factor of poor dielectric properties.

In contrast, as shown in Table 1, the pure $BaTiO_3$ with density of 5.47 g cm^{-3} (91.0%) and 5.10 g cm^{-3} (85.0%) showed dielectric constant of 1892 and 1657, respectively, at room temperature. These dielectric constant values are higher than those of tin-doped $BaTiO_3$ with similar relative densities (1421 and 1201 for $Ba_{0.9}Sn_{0.1}TiO_3$ and $Ba_{0.8}Sn_{0.2}TiO_3$).

These results indicated that the doping of tin in the lattice of $BaTiO_3$ gave evident effects on its various properties, including morphology, particle size and dielectric properties. Though the dielectric properties could not be improved through doping of tin in this paper, it is expected to improve some properties such as visible light absorption ability by optimizing the doping amount of tin since the color of samples changed significantly by doping with tin. Such properties are now under investigation.

Conclusions

Nanoparticles of barium titanate doped with Sn^{2+} were obtained by using a microwave-assisted solvothermal reaction. The Sn^{2+}-doped samples consisted of a single cubic perovskite phase. It was considered that Sn^{2+} entered into A site of the perovskite formula, ABO_3, because the lattice parameters decreased with increasing the amount of doped Sn^{2+}. The particle sizes were about 20–40 nm and increased with increasing the amount of doped Sn^{2+}. SPS method under an inert gas atmosphere has proved to be useful for the sintering of Sn^{2+}-doped $BaTiO_3$ to avoid the disproportionation reaction of Sn^{2+} at high temperature. The $BaTiO_3$, $Ba_{0.9}Sn_{0.1}TiO_3$ and $Ba_{0.8}Sn_{0.2}TiO_3$ samples sintered using a SPS method around 1100 °C with applying a pressure of 40 MPa showed dielectric constant of 2937, 1421 and 1201, respectively.

Acknowledgements This research was partially supported by the Ministry of Education, Culture, Sports, Science and Technology, Scientific Research of the Special Education and Research Expenses on "Post-Silicon Materials and Devices Research Alliance" and the JSPS Asian Core Program "Interdisciplinary Science of Nanomaterials".

References

1. Hosogi Y, Shimodaira Y, Kato H, Kobayashi H, Kudo A (2008) Chem Mater 20:1299. doi:10.1021/cm071588c
2. Mizoguchi H, Wattiaux A, Kykyneshi R, Tate J, Sleight AW, Subramanian MA (2008) Mater Res Bull 43:1943. doi:10.1016/j.materresbull.2008.03.011
3. Hosogi Y, Tanabe K, Kato H, Kobayashi H, Kudo A (2004) Chem Lett 33:28. doi:10.1246/cl.2004.28

4. Xie YH, Yin S, Yamane H, Hashimoto T, Machida H, Sato T (2008) Chem Mater 20:4931. doi:10.1021/cm800277b
5. Nagakai N, Oba N (2002) Japanese patent P2002-29838A
6. Konishi Y, Ohsawa M, Yonezawa Y, Tanimura Y, Chikyow T, Wakisaka T, Koinuma H, Miyamoto A, Kubo M, Sasata K (2003) Materials research society symposia proceedings vol 748, p U3.13.1
7. Konisi Y (2003) Japanese patent 2003-146660A
8. Koinuma H (2004) Japanese patent P2004-353072A
9. Koinuma H, Yonezawa Y (2005) Japanese patent P2005-259393A
10. Konisi Y, Osawa M, Yonezawa Y (2003) Fuji Jiho 76(4):241 (in Japanese)
11. Polla DL, Lorraine FF (1998) Annu Rev Mater Sci 28:563. doi:10.1146/annurev.matsci.28.1.563
12. Takenaka T, Nagata H (2005) J Eur Ceram Soc 25:2693. doi:10.1016/j.jeurceramsoc.2005.03.125
13. Yin S, Fujishiro Y, Sato T (1996) Br Ceram Trans 95:258
14. Yin S, Sato T (2000) Ind Eng Chem Res 39:4526. doi:10.1021/ie000165g
15. Yin S, Inoue Y, Uchida S, Fujishiro Y, Sato T (1998) J Mater Res 13:844. doi:10.1557/JMR.1998.0111
16. Anderson D, Virginia STC (2003) Chem Mater 15:1344. doi:10.1021/cm0210187
17. Sato T, Yin S, Xie YH (2007) Japanese patent P2007-155995A
18. Khor KA, Cheng KH, Yu LG, Boey F (2003) Mater Sci Eng A 347:300. doi:10.1016/S0921-5093(02)00601-9
19. Li W, Gao L (2000) J Eur Ceram Soc 20:2441. doi:10.1016/S0955-2219(00)00152-7
20. Ji G, Grosdidier T, Bozzolo N, Launois S (2007) Intermetallics 15:108. doi:10.1016/j.intermet.2006.03.006
21. Prakash BS, Varma KBR (2007) J Solid State Chem 180:1918. doi:10.1016/j.jssc.2007.04.018
22. Forrester JS, Zobec JS, Phelan D, Kisi EH (2004) J Solid State Chem 177:3553. doi:10.1016/j.jssc.2004.06.005
23. Boulos M, Fritsch SG, Mathieu F, Durand B, Lebey T, Bley V (2005) Solid State Ionics 176:1301. doi:10.1016/j.ssi.2005.02.024
24. Takahashi H, Numamoto Y, Tani J, Matsuta K, Qiu J, Tsurekawa S (2006) Jpn J Appl Phys 45:L30. doi:10.1143/JJAP.45.L30